Progress In Electromagnetics Research M, Vol. 54, 175–182, 2017

Studies on the Effect of Angle of Attack on the Transmission of Terahertz Waves in Reentry Plasma Sheaths

Kai Yuan, Ming Yao, Linfang Shen, Xiaohua Deng*, and Lujun Hong

Abstract—The communication 'blackout' in the reentry stage of a space mission is a serious threat to the reentry vehicle. The terahertz (THz) technology is supposed to be a potential solution to the 'blackout' problem in the recent decade. In the present paper, the relation between the THz waves' transmission in the reentry plasma sheath and the angle of attack (AOA) of the vehicle is investigated. A three-dimensional numerical model is introduced in order to obtain the plasma parameters in the reentry plasma sheaths. The computation results show that both the electron density and the electron collision frequency vary with the AOA. As results, the transmission rates for the THz waves vary with the AOA as well. According to the analysis, microwave communication system is very likely to suffer from the 'blackout' in the reentry stage. The THz scheme is an effective solution. The fluctuation of AOA may weaken the signal strength received by the onboard antenna. On the other hand, keeping the AOA in an appropriate range is helpful for strengthening the received THz signals. Also, the AOA for the best THz communication quality is obtained according to the analysis.

1. INTRODUCTION

Once a vehicle is moving hypersonically in the near space, the shock in front of the vehicle leads to aerothermal heating on the gas surrounding the vehicle. The neutral gas is ionized due to the high temperature. As a result, a dense plasma sheath is formed. The electron density in the plasma sheath can be up to $10^{20}\,\mathrm{m}^{-3}$, and the corresponding cutoff frequency is 89.8 GHz. If the frequency of the radio wave is lower than the cutoff frequency, the radio wave will be blocked by the dense plasma sheath, then the so-called 'blackout' occurs.

The 'blackout' leads to risks of mission failure. Particularly, it is a serious threat to astronauts' lives in manned space missions. Despite that there is not any general solution to the 'blackout', so far, many approaches have been presented since 1950s. In the recent decade, the terahertz (THz) technology have become one of the hottest research topics, due to its high application capabilities [1, 2]. In space engineering, the THz scheme is considered to be a potential solution to the 'blackout' problem. Usually, the THz wave means the wave frequency in the band from 10^{11} Hz to 10^{13} Hz (0.1 THz to 10 THz).

In recent years, many scientists have paid attention to the transmission properties of THz waves in dense plasma. Ai et al. studied the electromagnetic scattering of THz waves in inhomogeneous cylindrical plasma [3]. Yuan et al. investigated the transmission properties of THz waves in unmagnetized plasma slabs. They found that plasma density, electron collision frequency, temperature and thickness of the plasma slab made significant impact on the transmission properties of THz waves [4]. Tian et al. investigated the relation between the inhomogeneity of the plasma slab and the transmission properties of the THz waves [5]. Another noticeable work is the theoretical and experimental study on the transmission properties of Thz waves in plasma slabs in [6]. According to the study, the transmission of THz waves in plasma slabs is significantly influenced by the thickness of the plasma slab, electron

Received 25 December 2016, Accepted 8 February 2017, Scheduled 22 February 2017
* Corresponding author: Xiaohua Deng (deng_x_h@163.com).
The authors are with the Institute of Space Science and Technology, Nanchang University, Nanchang, Jiangxi Province 330031, China.

density profile and collision frequency profile. Moreover, Li et al. presented the theory about the THz data transmission system for reentry vehicles [7]. Those works remarkably deepen our knowledge about the transmission properties of THz waves in dense plasma.

On the other hand, those works used to be carried out based on presumed plasma slabs. Unfortunately, a realistic plasma sheath is much more complicate than presumed plasma slabs. For a presumed plasma slab, the plasma parameters are given, and each parameter varies independently. Since the reentry is a dynamic process, the parameters of a reentry plasma sheath vary simultaneously. Those parameters depend on the aerodynamic shape and flight condition of the vehicle [8, 9]. The factors which significantly impact the THz waves' transmission in a realistic plasma sheath are not identical to those in presumed plasma slabs [10]. Therefore, in order to solve the 'blackout' problem with THz scheme, it is necessary to study the transmission properties of THz waves in realistic plasma sheaths rather than that in presumed plasma slabs.

Recently, Jung et al. performed three-dimensional simulations for two reentry experiments, which are the Orbital Reentry Experiment (OREX) by Japan and the Atmospheric Reentry Demonstrator (ARD) by ESA [11]. The simulation results showed good agreement with the experimental data. Additionally, two angles of attack (AOA) for the ARD experiment, which are 0° and 20°, have been investigated. The study revealed that the AOA significantly influenced the distributions of both the electron density and temperature in the plasma sheath. The AOA of the ARD vehicle helps to maintain the communication with the tracking and data relay satellites (TDRS) in the reentry stage. However, Jung et al. only considered the microwave communication in the study.

In the present study, the dependence of the THz waves' transmission on the AOA is considered. The reentry plasma sheath of the RAMC-II vehicle, which is a blunt coned object, is taken for example in the present study. A three-dimensional hypersonic fluid model is introduced in order to obtain the plasma parameters in the reentry plasma sheaths. And then the transmission rates for the THz waves in the plasma sheaths are calculated with the analytic theory. Also, the application of the AOA to THz communication in reentry missions is discussed.

2. THE HYPERSONIC FLUID MODEL

The reentry plasma sheath is obtained by solving a three-dimensional single fluid multi-species model. The model is developed based on the Navier-Stokes (N-S) equations and gas molecular theories [10, 12, 13]. The conservative form for the N-S equations is given below:

$$\frac{\partial \rho}{\partial t} + \nabla \cdot (\rho \vec{u}) = 0 \tag{1}$$

$$\frac{\partial (\rho \vec{u})}{\partial t} + \nabla \cdot \left(\rho \vec{u} \otimes \vec{u} + p \vec{\vec{I}} \right) = \nabla \cdot \vec{\vec{\tau}} \tag{2}$$

$$\frac{\partial e}{\partial t} + \nabla \cdot [\vec{u} (e + p)] = \nabla \cdot \left(\vec{\vec{\tau}} \cdot \vec{u} \right) + \nabla \cdot (k_T \nabla T) \tag{3}$$

Table 1. Nomenclature. All the variables are in SI unit system.

ρ: mass density	t: time	n: number density
p: pressure	e: total energy	m: mass
R: gas constant	T: temperature	μ: dynamic viscosity
H: enthalpy of formation	σ: collision diameter	k_T: thermal conductivity
Ω: collision integral	k_B: Boltzmann constant	Pr: Prandtl number
f: degrees of freedom	N: total number of species	s: source of species
ν_e: electron collision frequency	γ: c_P/c_V	c_P: specific heat at constant pressure
c_V: specific heat at constant volume	$\vec{u}$: fluid velocity	i: subscript, the i-th species
$\vec{\vec{\tau}}$: viscous stress tensor	$\vec{\vec{I}}$: unit tensor	

All the variables are defined in Table 1. Equations (1), (2) and (3) are the mass conservation equation, momentum conservation equation and energy conservation equation, respectively. The mass density and pressure are defined as $\rho = \sum_i^N n_i m_i$ and $p = \rho RT$, respectively. The expression for the viscous stress tensor is:

$$\vec{\vec{\tau}} = -\frac{2}{3}\mu\left(\nabla \cdot \vec{u}\right)\vec{\vec{I}} + \mu\left[\nabla \otimes \vec{u} + \left(\nabla \otimes \vec{u}\right)^T\right] \tag{4}$$

where superscript T is the transpose operator. The total energy is defined as:

$$e = \frac{p}{\gamma - 1} + \frac{1}{2}\rho\vec{u} \cdot \vec{u} + \sum_i^N n_i H_i \tag{5}$$

The three terms on the right are thermal energy, kinetic energy of fluid and chemical energy, respectively.

In order to close the system of equations for the model, the number density continuity equation is introduced:

$$\frac{\partial n_i}{\partial t} + \nabla \cdot \left(n_i \vec{u}\right) = s_i \tag{6}$$

And the rest of necessary variables, given below, are derived from gas kinetic theories [12, 14].

$$\mu_i = \frac{5}{16}\frac{\sqrt{\pi m_i k_B T}}{\pi\sigma^2\Omega} \tag{7}$$

$$c_{Pi} = \left(\frac{f}{2} + 1\right) R_i \tag{8}$$

$$c_{Vi} = c_{Pi} - R_i \tag{9}$$

$$k_{Ti} = \frac{5}{2} c_{Vi}\mu_i \tag{10}$$

The source term in Equation (6), which represents the chemical reactions in the plasma sheath, is given by the air 7-species model. The air 7-species model was developed by NASA. σ, Ω, f, c_{Pi} and c_{Vi} in Equations (7) to (10) are given by the 7-species model as well.

The hypersonic fluid model is solved numerically in an unstructured mesh with the FVM method. The reentry body in the present study is a RAMC-II shaped vehicle, which is a rotational symmetric blunt coned object. The nose cap radius of the vehicle is 15.24 cm, and the half angle is 9°. The length of the vehicle is 1.29 m [15, 16]. In the present study, the altitude of the vehicle is 31 km. The reentry speed is 6550 m/s, which is identical to the RAMC-II experiment at the same altitude. Since the AOA of the ARD experiment is 20° [11], the range of the AOA concerned in the present study is from 0° to 30°.

3. RESULTS AND DISCUSSION

3.1. The Reentry Plasma Sheath

An example of the plasma sheath is shown in Fig. 1. The AOA for the example is 15°. The vehicle is at rest with respect to the reference frame in the present study. The electron collision frequency is calculated in accordance with the equation derived by Lankford [17], which is given below:

$$\nu_e = 5.814 \times 10^{12}\frac{p}{p_0\sqrt{T}} \tag{11}$$

where p_0 is the standard atmospheric pressure, and $p = \rho RT$. Therefore,

$$\nu_e = 5.814 \times 10^{12}\frac{\rho R\sqrt{T}}{p_0} \tag{12}$$

The clip views for the electron density (N_e) and electron collision frequency (ν_e) are illustrated in Fig. 1(a) and Fig. 1(b), respectively. The main axis of the vehicle is parallel to the x axis. The height and bottom radius of the simulation box, which is a frustum of cone, are 2.5 m and 1.0 m, respectively. The blunt coned holes in the centers of the two plots represent the body of the vehicle. For the nonzero

AOA, it can be expected that the plasma sheath is no longer rotational symmetric. In the present study, the plasma distributions in the regions of $y > 0$ and $y < 0$ are not identical while AOA $\neq 0°$. According to Fig. 1(c) and Fig. 1(d), both the electron density and collision frequency in the region of $y > 0$ are obviously smaller than those in the region of $y < 0$. Therefore, it makes sense to install the antenna on the wall in the region of $y > 0$. In the current reference of frame, the antenna is in the x-y plane. Its axial distance to the nose cap of the vehicle is 0.8 m. The dependence of the parameters on the AOA near the antenna is illustrated in Fig. 2.

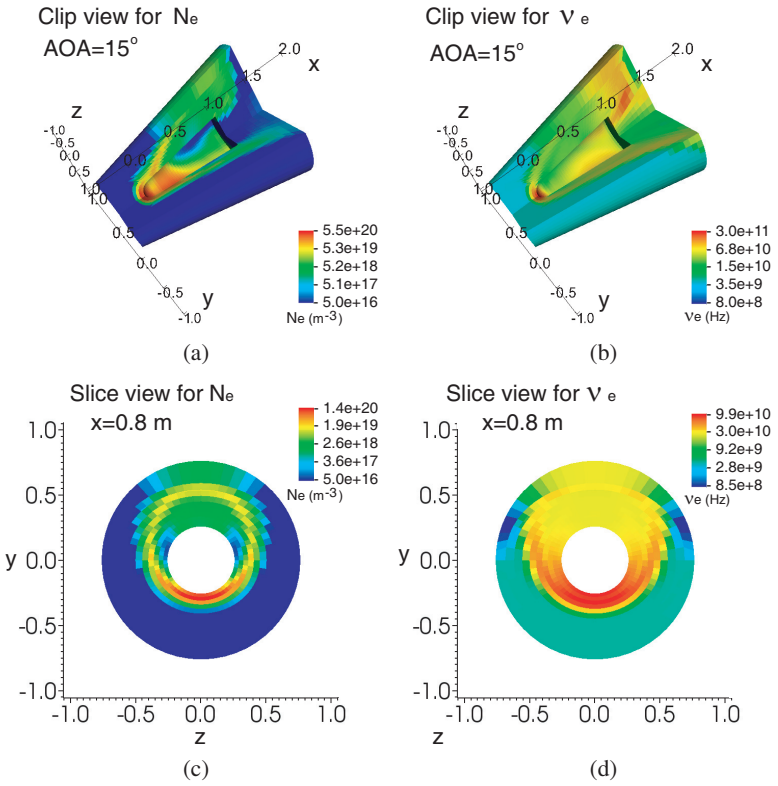

Figure 1. Clip and slice views for the N_e and ν_e.

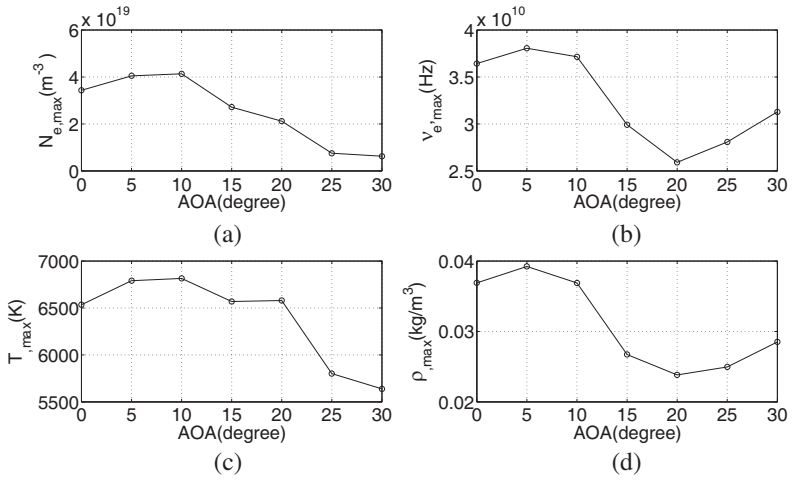

Figure 2. The dependence of the parameters on the AOA near the antenna.

Figures 2(a) and 2(b) show that the electron density slightly increases with the AOA until the AOA reaches 10°. Once AOA > 10°, the electron density decreases with the AOA. The electron collision frequency slightly increases with the AOA while 0° ≤ AOA ≤ 5°. Once AOA > 5°, the collision frequency decreases with the AOA in the range from 5° to 20°, and then it increases with the AOA while AOA > 20°. Such variations may be caused by the flow properties in the plasma sheath.

The velocity of the shock is always in the x-y plane in the present study. The shock velocity component in the y-direction (v_y) is zero while AOA = 0°. In such a case, there are two main sources for the plasma near the antenna. The ionization near the antenna due to the high temperature is one of the sources. The other source is the plasma flow from the region near the nose cap. According to Fig. 1(a), the electron density near the wall generally decreases with the axial distance to the nose cap in the region of $x > 0$. Therefore, the flow brings the plasma in the region near the nose cap into the regions beyond the nose cap. However, for the cases of AOA ≠ 0°, $v_y > 0$. The nonzero v_y leads to the flow perpendicular to the main axis of the vehicle. As a result, the fluid flows over the vehicle not only from the nose cap to the bottom of the vehicle but also from the region of $y < 0$ to the region of $y > 0$. According to Fig. 1(c), the plasma in the region of $y < 0$ is denser than that in the region of $y > 0$. Hence the flow over the vehicle brings the plasma in the region of $y < 0$ into the region of $y > 0$. It is the reason that the electron density slightly increases with the AOA in the range from 0° to 10°.

On the other hand, the electron density decreases with the AOA while AOA > 10°. The reason may be that v_y increases with the AOA, while v_x decreases with the AOA. Since y component of the moving shock is partially shielded by the body of the vehicle in the region of $y < 0$, and the component along the x direction gets weaker when the AOA increases, the aerothermal heating near the antenna is weakened. As a result, the ionization in the region of $y > 0$ is weakened and the electron density decreased.

Despite that the electron density near the antenna decreases, the electron collision frequency increases with the AOA while AOA > 20°. According to Fig. 2(b) and Fig. 2(d), the mass density near the antenna makes significant impact. The mass density variation with the AOA is led by the complex nonlinear convection in the plasma sheath (e.g., the turbulent vortices), particularly in the region near or in the wake [18]. Due to its complexity, such nonlinear convection in the plasma sheath will be left for future research tasks.

3.2. The Transmission of THz Waves

In a reentry plasma sheath, the spatial scale of the plasma parameter variation is much smaller than the wavelength of THz waves. In such a case, the transmission rate of THz waves can be obtained with the WKB approximation. In the present study an analytic theory of EM wave propagation is utilized [19, 20]. The propagation of EM wave in the plasma sheath is expressed as given below:

$$\gamma_p(l) = \alpha_p(l) - j\beta_p(l) \tag{13}$$

where l is the distance to the outer boundary of the plasma sheath.

$$\alpha_p(l) = k_0\sqrt{\left\{\left[K_r(l)^2 + K_i(l)^2\right]^{1/2} - K_r(l)\right\}/2} \tag{14}$$

$$\beta_p(l) = k_0\sqrt{\left\{\left[K_r(l)^2 + K_i(l)^2\right]^{1/2} + K_r(l)\right\}/2} \tag{15}$$

$$K_r = 1 - \frac{f_p(l)^2}{f^2 + \nu(l)^2} \tag{16}$$

$$K_i = \frac{f_p(l)^2\left[\nu(l)/f\right]}{f^2 + \nu(l)^2} \tag{17}$$

where k_0 is the wave number. The wave transmission is as given below:

$$E_t/E_0 = \exp\left[-\int_0^L (\gamma_p)\, dl\right] \tag{18}$$

where L is the length of the transmission path. The incident angle of the waves in the present study is 0°; therefore, tL is the thickness of the plasma sheath near the antenna. Fig. 3 illustrates the dependence of the THz wave transmission on the AOA.

The concerned wave frequencies in the present study are 0.1 THz, 0.22 THz and 0.3 THz, respectively. 0.1 THz is the minimum frequency of the THz band. Also, the wave of 96 GHz, which is very close to 0.1 THz, is involved in a ground experiment [21]. 0.22 THz is involved in another ground experiment by Zheng et al. [6]. 0.3 THz is the carrier frequency of a successful wireless THz data transmission system [22]. According to Fig. 3, the transmission rates (T_p) for all the frequencies decrease with the AOA while $0° \leq \text{AOA} \leq 5°$. Once AOA $> 5°$, the T_p increases with the AOA till the AOA reaches 25°. And then T_p decreases with the AOA while AOA $> 25°$.

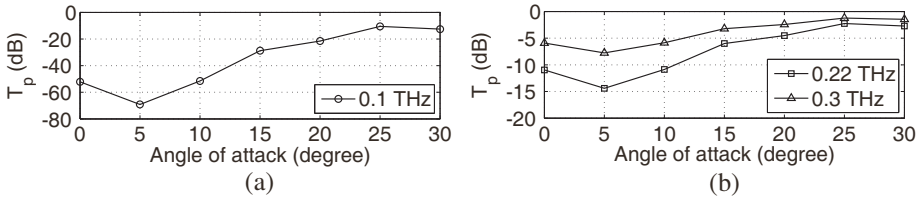

Figure 3. The transmission rates vs. the AOA for the waves of (a) 0.1 THz, (b) 0.22 THz and 0.3 THz.

For a space mission, the AOA may fluctuate during the reentry stage. For example, in the RAMC-II reentry experiment, the payload measurements showed that the AOA fluctuated in the range from 0° to 6° [15]. On the other hand, it should be noticed that the T_p at AOA = 10° is almost equal to the T_p at AOA = 0°, and the T_p at AOA = 5° is smaller than that of AOA = 0°. It indicates that the transmission rate for THz waves will be weakened if the AOA fluctuates in the range from 0° to 10°. In other words, the communication quality may get worse if the AOA fluctuates in the range from 0° to 10°. On the other hand, the T_p for all the frequencies are higher than that of zero AOA once AOA $> 10°$. Therefore, to keep the AOA greater than 10° is helpful for strengthening the THz signals received by the antenna. In other words, the communication quality can be improved by keeping the AOA greater than 10°.

Furthermore, the transmission rate for the waves of 0.1 THz is rather poor once the AOA is smaller than 15°. In the present study, the criterion for the 'blackout' is assumed to be $T_p \leq -20$ dB. In such a case, if the carrier frequency for the THz communication system is 0.1 THz, the AOA should be greater than 20° in order to mitigate the 'blackout' effectively (see Fig. 3(a)). Also, it is indicated that a microwave communication system is very likely to suffer from the 'blackout' during the reentry stage. On the other hand, according to Fig. 3(b), if the carrier frequency is 0.22 THz or 0.3 THz, the 'blackout' can always be mitigated effectively. Therefore, the THz communication technology is an effective solution to the 'blackout' problem.

Moreover, the T_p for waves of 0.3 THz is obviously greater than that of 0.22 THz, particularly in the cases of AOA $\leq 15°$. It is suggested that to utilize a higher carrier frequency can effectively enhance the transmission rate for the THz signals once the AOA is relatively small. Additionally, once the AOA is greater than 5°, increasing the AOA can strengthen the THz signal received by the antenna. As a result, the communication quality is improved. However, since T_p slightly decreases with the AOA once AOA $> 25°$, it is not necessary to further increase the AOA once the AOA reaches 25°. In other words, the AOA for the best THz communication quality in a reentry mission is 25°.

4. SUMMARY AND CONCLUSION

In the present study, the structure of the plasma sheath for an RAMC-II shaped reentry vehicle is investigated numerically based on a three-dimensional hypersonic fluid model. The impacts led by the AOA are investigated. The antenna is assumed to be installed on the wall of the vehicle. The transmission rate of THz waves near the antenna is investigated. The frequencies concerned are 0.1 THz, 0.22 THz and 0.3 THz, respectively.

The conclusions are:

1. The AOA significantly impacts the electron density and the electron collision frequency near the wall of the reentry vehicle. As a result, T_p varies with AOA as well.
2. The microwave communication is very likely to suffer from the 'blackout'. The THz scheme is an effective solution to the 'blackout' problem.
3. Compared with the case of zero AOA, the received signal strength will be weakened if the AOA fluctuates in the range from 0° to 10°.
4. Keeping the AOA larger than 10° is helpful for strengthening the THz signal received by the onboard antenna.
5. In the reentry stage, the AOA for the best THz communication quality is 25°.

ACKNOWLEDGMENT

This work was supported by Jiangxi Postdoctoral Grant (Award No. 2013KY43) and Natural Science Foundation of Jiangxi Province (Award No. 20151BAB207004).

REFERENCES

1. Viti, L., D. Coquillat, A. Politano, K. A. Kokh, Z. S. Aliev, M. B. Babanly, O. E. Tereshchenko, W. Knap, E. V. Chulkov, and M. S. Vitiello, "Plasma-wave terahertz detection mediated by topological insulators surface states," *Nano Letters*, Vol. 16, No. 1, 80, 2016.
2. Viti, L., J. Hu, D. Coquillat, A. Politano, W. Knap, and M. S. Vitiello, "Efficient terahertz detection in black-phosphorus nano-transistors with selective and controllable plasma-wave, bolometric and thermoelectric response," *Scientific Reports*, Vol. 6, 2016.
3. Ai, X., Y. Tian, Z. Cui, Y. Han, and X.-W. Shi, "A dispersive conformal FDTD technique for accurate modeling electromagnetic scattering of THz waves by inhomogeneous plasma cylinder array," *Progress In Electromagnetics Research*, Vol. 142, 353–368, 2013.
4. Yuan, C.-X., Z.-X. Zhou, J. W. Zhang, X.-L. Xiang, F. Yue, and H.-G. Sun, "FDTD analysis of terahertz wave propagation in a high-temperature unmagnetized plasma slab," *IEEE Transactions on Plasma Science*, Vol. 39, No. 7, 1577–1584, 2011.
5. Tian, Y., Y. Han, Y. Ling, and X. Ai, "Propagation of terahertz electromagnetic wave in plasma with inhomogeneous collision frequency," *Physics of Plasmas*, Vol. 21, No. 2, 023301, (1994-present), 2014.
6. Zheng, L., Q. Zhao, S. Liu, X. Xing, and Y. Chen, "Theoretical and experimental studies of terahertz 219 wave propagation in unmagnetized plasma," *Journal of Infrared, Millimeter, and Terahertz Waves*, Vol. 35, No. 2, 187–197, 2014.
7. Li, J., Y. Pi, and X. Yang, "A conception on the terahertz communication system for plasma sheath penetration," *Wireless Communications and Mobile Computing*, Vol. 14, No. 13, 1252–1258, 2014.
8. Starkey, R. P., "Hypersonic vehicle telemetry blackout analysis," *Journal of Spacecraft and Rockets*, Vol. 52, No. 2, 426–438, 2015.
9. Meyer, J. W., "System and method for reducing plasma induced communication disruption utilizing electrophilic injectant and sharp reentry vehicle nose shaping," US Patent 7237752, 2007.
10. Chen, J., K. Yuan, L. Shen, X. Deng, L. Hong, and M. Yao, "Studies of terahertz wave propagation in realistic reentry plasma sheath," *Progress In Electromagnetics Research*, Vol. 157, 21–29, 2016.
11. Jung, M., H. Kihara, K. I. Abe, and Y. Takahashi, "Numerical analysis on the effect of angle of attack on evaluating radio-frequency blackout in atmospheric reentry," *Journal-Korean Physical Society*, Vol. 68, No. 11, 1295–1306, 2016.
12. Kundrapu, M., J. Loverich, K. Beckwith, and P. Stoltz, "Electromagnetic wave propagation in the plasma layer of a reentry vehicle," *IEEE International Conference on Plasma Sciences*, 1–4, 2014.
13. Kundrapu, M., J. Loverich, K. Beckwith, P. Stoltz, A. Shashurin, and M. Keidar, "Modeling radio communication blackout and blackout mitigation in hypersonic vehicles," *Journal of Spacecraft and Rockets*, Vol. 52, No. 3, 853–862, 2015.

14. Gupta, R. N., J. M. Yos, R. A. Thompson, and K.-P. Lee, "A review of reaction rates and 241 thermodynamic and transport properties for an 11-species air model for chemical and thermal nonequilibrium calculations to 30000 K," *NASA STI/Recon Technical Report N*, Tech. Rep., Aug. 1990.
15. Grantham, W. L., "Flight results of a 25000-foot-per-second reentry experiment using microwave reflectometers to measure plasma electron density and standoff distance," Tech. Rep., NASA TN D-6062, Washington, D. C., Dec. 1970.
16. Jones, Jr., W. L. and A. E. Cross, "Electrostatic-probe measurements of plasma parameters for two reentry flight experiments at 25000 feet per second," Tech. Rep., NASA TN D-6617, Washington, D. C., Feb. 1972.
17. Lankford, D. W., "A study of electron collision frequency in air mixtures and turbulent boundary," Tech. Rep., DTIC Document AFWL-TR-72-71, Oct. 1972.
18. Reddy, D. S. K. and K. Sinha, "Hypersonic turbulent flow simulation of Fire II reentry vehicle afterbody," *Journal of Spacecraft and Rockets*, Vol. 46, No. 4, 745–757, 2009.
19. Rybak, J. P. and R. J. Churchill, "Progress in reentry communications," *IEEE Transactions on Aerospace Electronic Systems*, Vol. 7, No. 5, 879–894, 1971.
20. Mehra, N., R. K. Singh, and S. C. Bera, "Mitigation of communication blackout during re-entry using static magnetic field," *Progress In Electromagnetics Research B*, Vol. 63, 161–172, 2015.
21. Zheng, L., Q. Zhao, S. Liu, P. Ma, C. Huang, Y. Tang, X. Chen, X. Xing, C. Zhang, and X. Luo, "Theoretical and experimental studies of 35 GHz and 96 GHz electromagnetic wave propagation in plasma," *Progress In Electromagnetics Research M*, Vol. 24, 179–192, 2012.
22. Jastrow, C., S. Priebe, B. Spitschan, J.-M. Hartmann, M. Jacob, T. Kurner, T. Schrader, and T. Kleine-Ostmann, "Wireless digital data transmission at 300 GHz," Electronics Letters, Vol. 46, No. 9, 661–663, 2010.